

S⁴R: Self-Supervised Semantic Scene Reconstruction from RGB-D Scans

Junwen Huang¹ Alexey Artemov¹ Yujin Chen¹ Shuaifeng Zhi^{2*} Kai Xu² Matthias Nießner¹

¹Technical University of Munich ²NUDT

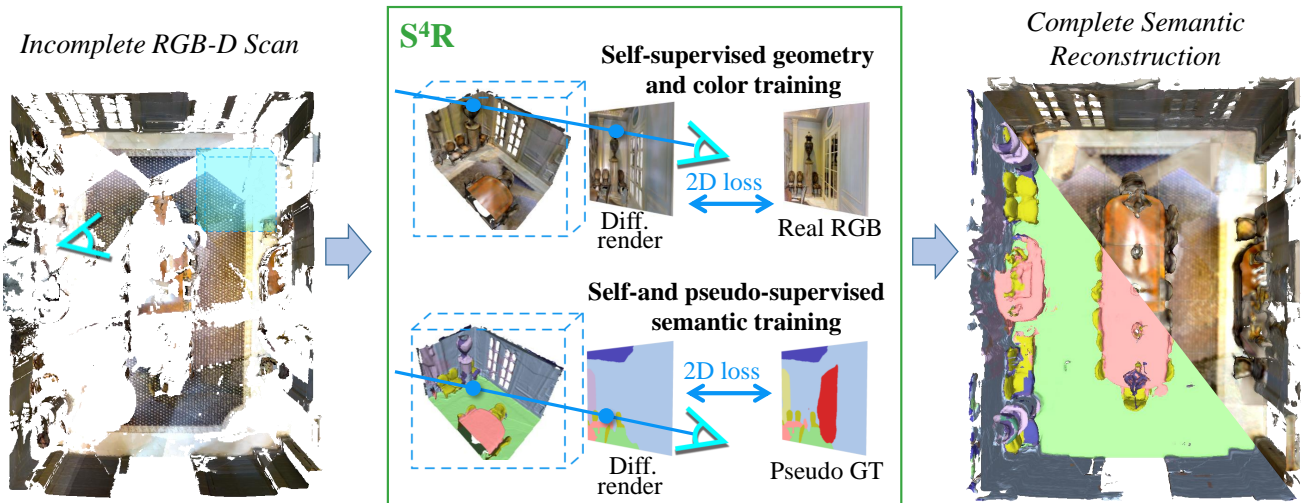


Figure 1. Given sparse RGB-D images, our method is capable of jointly predicting complete geometry, appearance, and semantic labels without access to any 3D or 2D in-place ground-truth annotations during training.

Abstract

Most deep learning approaches to comprehensive semantic modeling of 3D indoor spaces require costly dense annotations in the 3D domain. In this work, we explore a central 3D scene modeling task, namely, semantic scene reconstruction, using a fully self-supervised approach. To this end, we design a trainable model that employs both incomplete 3D reconstructions and their corresponding source RGB-D images, fusing cross-domain features into volumetric embeddings to predict complete 3D geometry, color, and semantics. Our key technical innovation is to leverage differentiable rendering of color and semantics, using the observed RGB images and a generic semantic segmentation model as color and semantics supervision, respectively. We additionally develop a method to synthesize an augmented set of virtual training views complementing the original real captures, enabling more efficient self-supervision for semantics. In this work we propose an end-to-end trainable

solution jointly addressing geometry completion, colorization, and semantic mapping from a few RGB-D images, without 3D or 2D ground-truth. Our method is the first, to our knowledge, fully self-supervised method addressing completion and semantic segmentation of real-world 3D scans. It performs comparably well with the 3D supervised baselines, surpasses baselines with 2D supervision on real datasets, and generalizes well to unseen scenes.

1. Introduction

There seems to exist an agreement that accurate modeling of geometry, appearance, and semantics are three essential ingredients for the construction of comprehensive digital replicas for real-world 3D scenes. Indeed, downstream applications such as the creation and manipulation of 3D assets, virtual-real interactions, or free-viewpoint virtual tours all require complete 3D shapes and faithful color information of objects [3, 32]. Others, supporting autonomous systems to localize themselves, to navigate environments, or to

*Shuaifeng Zhi is the corresponding author.

perform tasks like grasping, involve understanding semantics and accurate modeling of scene geometry [7, 15].

Digitizing real-world 3D scenes such as entire indoor areas, however, is widely recognized as a challenging endeavor; limitations of range 3D scanning and physical constraints such as occlusions disable acquiring complete 3D geometry (see, *e.g.*, [12, 22]). Moreover, even resorting to human experts for either scanning, semantic annotation, or artistic editing is unlikely to deliver flawless, complete digital 3D assets while being notoriously labour-intensive [3, 9]. This view has motivated much research on automatic (particularly, learning-based) approaches for completion, colorization, and semantic segmentation of raw single-view [2, 14, 34, 36], multi-view [11, 24], and fused 3D acquisitions [12, 13, 21, 22].

Despite these efforts brought in methods capable of recovering one or two (“geometry + semantics” or “geometry + color”) of the target quantities from raw RGB-D scans independently, a comprehensive joint understanding of all three complementary signals has not been yet demonstrated. To address this gap, in this work we propose to jointly predict geometry, appearance, and semantics using a three-branch 3D CNN architecture, and empirically validate the feasibility of this scheme; to our best knowledge, our system is the first to predict the three complementary targets using a single trained model.

Training a multi-modal, highly parameterized 3D network in the 3D domain in a *fully supervised* manner is challenging as it depends on vast amounts of diverse, high-quality, complete, and labeled 3D data. Learning from purely synthetic data (*e.g.*, [31, 34]) is unlikely to well generalize to real 3D scans; on the other hand, ground-truth 2D/3D data and semantic annotation masks in common real-world RGB-D datasets (see, *e.g.*, [1, 3, 9]) are incomplete and imperfect. Instead, we opt for a number of design choices enabling our learning algorithm to leverage the original RGB-D images along with a generic semantic segmentation model [30] in a *self-supervised* fashion.

First, inspired by recent methods [10, 13], we remove a subset of RGB-D frames from the input and learn to predict a complete semantic scene from an incomplete reconstruction; for this, we design a three-branch deep 3D CNN to jointly output geometry, color, and semantics in each voxel. Second, to support end-to-end optimization of our learning-based algorithm, we develop an extended differentiable rendering method, enabling us to render 3D volume data to depth, RGB and semantic images through raycasting directly. We design our training algorithm to reproduce the original RGB-D data; as a key ingredient for learning semantics, we learn to replicate segmentations provided by a neural predictor generic on diverse, multi-domain data. Third, we additionally adapt the virtual view augmentation scheme inspired by the recent work [29] to further improve

training performance.

The direction we chose is in line with recent approaches where 2D view information is used to supervise 3D predictions [13, 17]. Our method can additionally be viewed as generalizing upon several recent works [10, 12, 13] by integrating RGB or semantic inputs as supervision; in several instances, we compare to these prior arts.

Our key contributions are as follows:

- To the best of our knowledge, we propose to date the first self-supervised approach to address semantic reconstruction of complex, real-world 3D indoor spaces.
- To free our method from any costly specific semantic annotations and enable self-supervised learning of a 3D CNN model, we extract semantic guidance from a generic deep network operating in the 2D image domain, extending the generality in more application scenarios for our method.
- To support efficient end-to-end training, we expand differentiable rendering with a subroutine to synthesize semantic images, building the gap between high-quality geometry reconstruction and 2D supervision.

2. Related Work

We briefly review closely related approaches that target analysis of large-scale, volumetric 3D scenes, mentioning works for other 3D representations where possible.

Semantic Scene Segmentation and its variants [19, 27] generally serve as in initial stage in scene analysis and continue to be extensively researched, in particular for RGB images (see, *e.g.*, [19, 26, 43] for a review). Yet, transferring 2D image segmentation to 3D world is non-straightforward; to this end, specialized point-, voxel-, and mesh-based methods were proposed (surveyed in [39]); we particularly note volumetric approaches [5, 9, 12, 37] as our network architecturally is a 3D CNN defined on a voxel grid. Seeking to empower 3D scene segmentation with image-based features, recent approaches propose multiple schemes to leverage 2D and 3D data in parallel [11, 17, 21, 24]. Among these, un-projecting per-pixel appearance features from nearby RGB-D images for 3D semantic [11] and 3D instance [21] segmentation and employing bidirectional view-voxel projection to mutually reinforce 2D and 3D features [24] proved to be effective. For 3D scenes represented as meshes, a more direct approach is to render and segment diversely sampled virtual 2D views using a pre-trained image-based network [29]; we adapt their view sampling scheme to our approach. All these approaches are fully supervised and require dense 3D annotation during training.

For reducing labeling costs and aiding generalization for 3D scene understanding, recent works sought to learn representations in a self-supervised fashion in a separate pre-training step (*e.g.*, [4, 23, 38]); however, these methods still

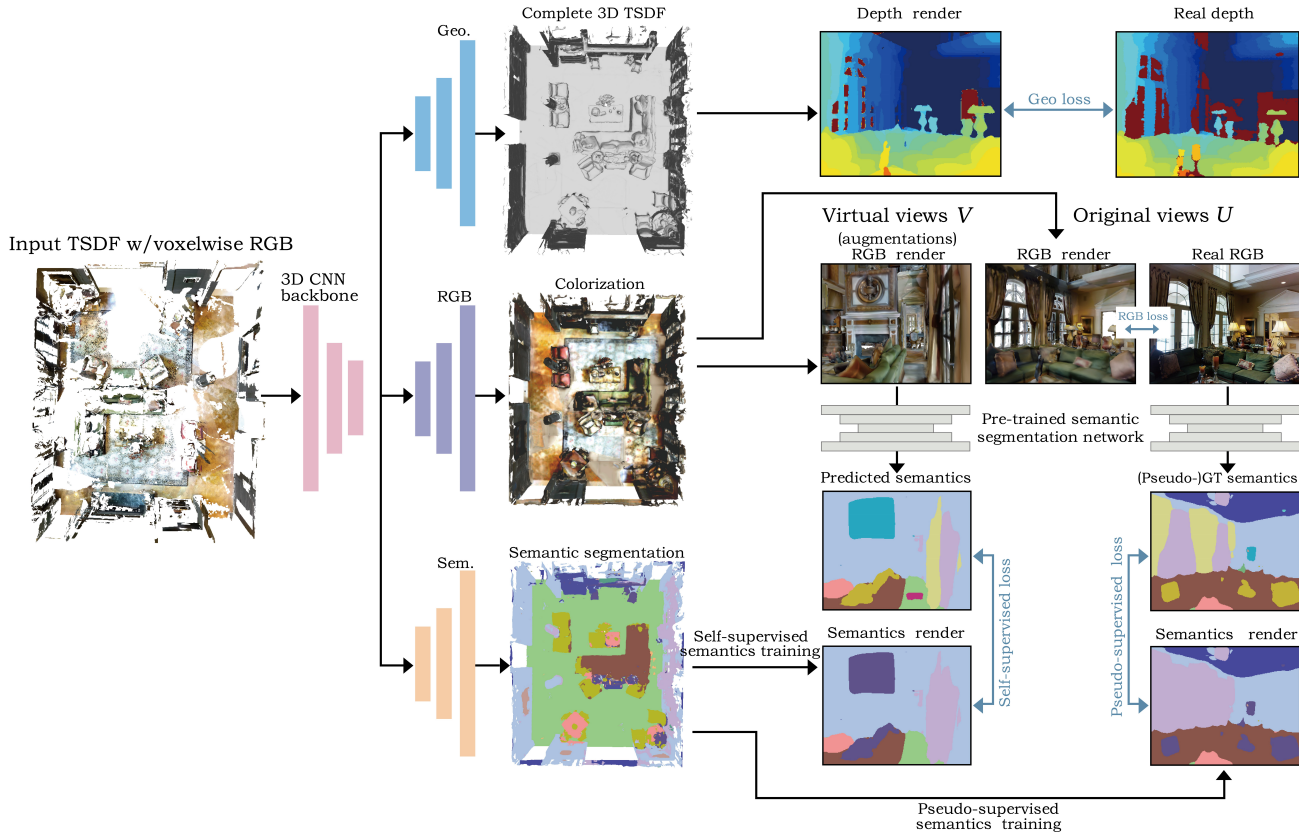


Figure 2. Our method accepts a fused but incomplete TSDF reconstruction as input and convolves it with a 3D encoder-decoder CNN, producing complete 3D geometry, colorization, and semantic segmentation. For end-to-end training, we generate 2D depth, color, and semantic images using either the original viewpoints U , or arbitrary virtual viewpoints V , by a differentiable rendering technique. These synthesized views are used to supervise training w.r.t. the original RGB-D images in a pseudo-supervised training loop, or w.r.t. multi-view consistency in a self-supervised training loop.

require 3D annotations for fine-tuning. Most similarly to our approach, 2D3DNet [17] obtains 2D features in each image using a pre-trained segmentation model, projects (“lifts”) these predictions to 3D points, and refines them by a 3D network trained without 3D labels, bypassing the need for 3D annotations during training. [33] predicts semantic segmentation for a target viewpoint by rendering a volumetric 3D representation of projected semantics predicted by a pre-trained segmentation model. Similarly to the latter two works, we use an existing pre-trained generic segmentation network but with a synthesized appearance view. All these approaches entirely leave out geometry completion or refinement, instead relying on raw scanned geometry.

Scene Completion. A common requirement in applications is to infer semantic labels not only in directly observed but also in occluded space; to this end, semantic scene completion [34] seeks to address both scene occupancy completion and semantic object labeling jointly. Single-view depth images can be viewed as minimal input data [18, 34–36, 41, 42]; alternatives [2, 12, 14, 22] (includ-

ing our method) tackle completing fused reconstructions of entire 3D spaces. [12] jointly predicts a truncated, unsigned distance field and per-volume semantics in a series of hierarchy levels ranging from low to high resolution. Leveraging RGB-D image back-projection, [22] combines geometry and appearance features to infer semantics and refine 3D geometry; [14] adopts a view of RGB image segmentation as a prior and computes the final semantic scene completion using a 3D CNN. [2] exploits an interplay between the scene- and instance-level completion tasks and alternates between semantic scene completion and detection of object instances. All these methods require dense 3D semantic labels and complete 3D reconstructions during training, making them dependent on synthetic datasets; in contrast, our algorithm is free from such restrictions as it trains from photometric losses obtained via appearance synthesis and an existing generic segmentation model in the 2D domain only.

Self-Supervised Scene Analysis. SG-NN [10] learns a scene completion network in a self-supervised learning task

where a more complete sparse truncated signed distance field (TSDF) volume is used to guide prediction with inputs from a less complete one. Most similarly to our work, SPSPG [13] diverts from using imprecise and incomplete 3D volumetric TSDF values as targets and leverages 2D appearance view synthesis where 2D image-based losses are used for supervising both completion and colorization. Our work presents an important extension of this line of research by enabling semantic segmentation in addition to generating complete and photometrically realistic scenes. Recently proposed semantics-enabled variants of neural radiance fields [16, 28, 44] strive to represent 3D scene geometry and semantics by a unified neural encoding; unlike these methods, our approach does not require expensive per-scene optimization and can generalize cross hundreds of unseen scenes.

3. Method

3.1. Method Overview

The goal of our method is to train a generalizable network g to perform semantic geometry completion, appearance (color) reconstruction, and semantic labeling without having access to the ground-truth (GT) annotations during training. The input to our method is a set of RGB-D frames $\{(I_u, D_u), u \in U\}$ and their respective estimated camera poses. To generate input reconstructions, we select a subset of views $\tilde{U} \subset U$, fusing these into a truncated signed distance field (TSDF) representation d_{in} through volumetric fusion [8], projecting color c_{in} to each voxel. As an output, our model predicts a corrected TSDF value \hat{d} , color \hat{c} , and semantic label \hat{s} in each voxel of the input grid.

Our network g follows a 3D encoder-decoder architecture with two encoders processing geometry and color, and three decoder branches to output geometry, appearance and semantic labels for each voxel (Section 3.2). Next, having computed predictions, we synthesize depth \hat{D}_v , appearance \hat{I}_v , and semantic \hat{S}_v views via a raytracing-based differentiable rendering process for TSDF volumes [13] (Section 3.3). To self-supervise training, we minimize a set of 2D losses involving the ground-truth image I_v , a pseudo-ground-truth semantic map S_v^p produced by a generic semantic segmentation model, and a synthetic semantic map \hat{S}_v^R generated via rendering (Section 3.4). For geometry completion, we additionally self-supervise training using the incomplete scan to produce a more complete scan. The network structure is shown in Figure 2 along with an overview of the training procedure.

3.2. Semantic Scene Reconstruction Architecture

We base our network architecturally on the variant proposed previously for photometric scene generation [13]. As input, our algorithm accepts a 4D tensor (*i.e.*, 3D volume

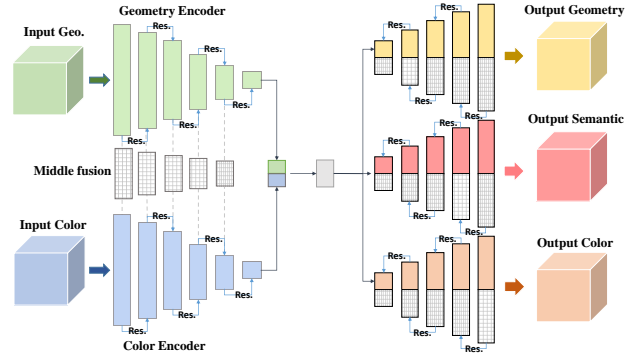


Figure 3. Our 3D CNN architecture comprises two encoders for geometry (geo.) and color, and three decoders for completed geometry, semantics, and color, respectively.

with per-voxel TSDF RGB values). To extract geometry and color features from each input volume, we use a backbone network with a dense 3D U-Net [6] design, comprised of two 3D encoder branches with 5 ResNet-type [20] convolutional blocks each, and three 3D decoder branches with an equal number of convolutional blocks in each.

For training, we extract subvolumes of input data from the scene-level 3D geometry and color data. First, we process these separately in parallel by 3D-convolving volumetric inputs with convolutional layers in the two encoders, gradually downsampling the input down to $c_v \times w \times h \times d$ feature volumes (we use $128 \times 8 \times 4 \times 4$ codes). At each block before downsampling, we additionally compute a stacked geometry/color feature map for passing to the respective upsampling blocks in the decoders. Next, the independently computed feature volumes are concatenated into a 4D feature map ($2c_v \times w \times h \times d$) and fused by a bank of convolutional layers to construct a joint latent feature space with the same shape. Finally, this fused feature volume is processed by three decoder branches independently to produce refined TSDF \hat{d} , color \hat{c} , and semantics \hat{s} values in each voxel. To enable better feature propagation at each level of the downsampling-upsampling hierarchy in the U-Net, we concatenate the color/geometry encodings to corresponding upsampling layers in the decoders. We present the full specification of our architecture in the supplemental.

Input and Network Varieties. We note a few important architectural differences w.r.t. the original SPSPG prototype [13], subject to available inputs; we leave details on training each variant for Section 3.4. The architecture of our 3D CNN is shown in Figure 3, where we summarise the data flow between the layers in our convolutional model.

In some instances, raw captured inputs cannot include color images but provide *depth only* $\{D_u\}$. Importantly, in this regime, colors can potentially assume arbitrary values (*e.g.*, walls in a room may be painted white or vividly

textured); hallucinating realistic appearance from geometry alone is a difficult generative problem and would require non-trivial complications to our model’s architecture (e.g., including an adversarial component). Instead, we opted to further simplify our model and make it entirely “color-blind” by removing 2D and 3D color encoders and decoders, disabling appearance synthesis during rendering (Section 3.3), and excluding RGB loss term (Section 3.4). Overall, we have found depth-only inputs to considerably decrease performance compared to RGB-D inputs.

3.3. Differentiable Rendering of Depth, Color and Semantics

Our key design choice is to train a network defined in 3D space, but leverage the information contained in the original 2D RGB-D images (possibly, augmented with semantic information) instead of relying on 3D annotation directly. We thus require a 3D-to-2D conversion to enable gradient flow from pixelwise to voxelwise representations. Such operations, known as *differentiable volumetric rendering* [25], have proven essential in multiple tasks (e.g., scene generation [13], surface reconstruction [40]). Among these ops, we opted to extend a straightforward, efficient raycasting-based rendering approach for TSDF volumes [13] with a subroutine to render semantic maps.

Our differentiable rendering algorithm \mathcal{R} accepts a predicted TSDF volume \hat{d} with per-voxel predicted colors \hat{c} and semantics \hat{s} and produces a set $\{\hat{D}_v = \mathcal{R}(\hat{d}; v), \hat{I}_v = \mathcal{R}(\hat{c}; v), \hat{S}_v = \mathcal{R}(\hat{s}; v)\}$ of depth, color and semantic images, respectively. To this end, we select RGB-D images taken from the viewing directions $\{v\}$ with the most overlap w.r.t. the chunk surface (top 5 views each with at least 5% depth samples within 2 cm to the near-surface voxels). For rendering semantics, we use a binary mask to represent each semantic class through raycasting, obtaining n_{sem} -channel one-hot semantics image where n_{sem} equals the number of semantic classes. Depth and color rendering are obtained using the original process from [13]. The resulting RGB color images contain three channels, and the semantic images contain n_{sem} channels, representing binary semantic masks for each of the semantic classes in the class taxonomy of the respective collection [3, 9]. Image resolution of synthesized views is 320×256 pixels.

Varying View Synthesis. Our system by default synthesizes depth, color, semantics views of the scene; however, to explore depth-only training, we disable color rendering and only produce depth and semantics. We note that as the predictions are assumed to be complete in 3D, one may use arbitrary viewing directions; we leverage this in our view augmentation technique (Section 4.1).

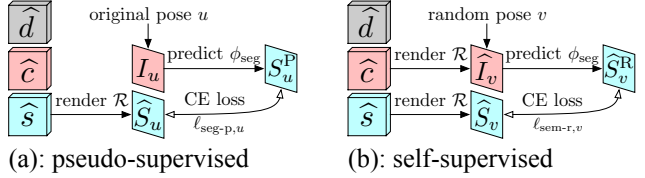


Figure 4. We optimize: (a) for the original views, deviations between segmented RGBs $\phi_{\text{seg}}(I_u)$ and same-view semantic renderings $\mathcal{R}(\hat{s}; u)$; (b) for randomly sampled views, deviations between semantic predictions of RGB renderings $\phi_{\text{seg}}(\mathcal{R}(\hat{c}; v))$ and direct semantic renderings $\mathcal{R}(\hat{s}; v)$ in the same view.

3.4. End-to-End Training with 2D Supervision

Our learning algorithm is conceptually inspired by SPSG [13], but differs from it in a number of ways, most importantly, by injecting semantic supervision and excluding adversarial components, which considerably simplifies our system. Similarly to SPSG though, our final scheme involves the objectives formulated in the 2D domain only, is end-to-end differentiable, and results in a 3D CNN model.

Geometry Completion. To self-supervise geometry completion, we use rendered depth images and penalize deviations from captured depth via pointwise L_1 loss

$$\ell_{\text{geo},u} = \sum_p \|D_u(p) - \hat{D}_u(p)\|_1. \quad (1)$$

We additionally use an L_1 3D loss term $\ell_{\text{geo-3d}}$ to self-supervise geometry reconstruction on the predicted 3D TSDF distances directly.

Appearance Reconstruction using Raw RGB Images. SPSG [13] heavily emphasized the need for adversarial training and optimizing a visual loss for achieving perceptually compelling RGB synthesis. In contrast, we opted to train without an adversarial part with either color or normal maps, hence bypassing the need for training a discriminator; likewise, to make the training task easier for the optimizer, we additionally exclude the perceptual loss term. Overall, we have found these modifications to have little effect on achieving high-quality completion or semantic segmentation while simplifying our system and bringing down the number of trainable parameters. As a result, to enable faithful color synthesis using our model, we simply minimize per-pixel L_1 distances between the synthesized appearance view \hat{I}_u and the target view I_u

$$\ell_{\text{app},u} = \sum_p \|I_u(p) - \hat{I}_u(p)\|_1. \quad (2)$$

Semantic Segmentation with 2D Supervision. The two types of our semantic losses follow a general intuition requiring that the segmentation \hat{s} inferred in the 3D domain generates plausible 2D semantic maps $\{\hat{S}_v\}$ under a certain

Method	Matterport3D		ScanNet	
	mAcc	mIoU	mAcc	mIoU
ScanComplete [12] (<i>sup.</i>)	34.9	28.2	29.5	22.7
3D CNN (<i>sup.</i>)	49.7	34.4	62.8	43.4
Ours (<i>self-sup., pseudo-GT</i>)	35.3	21.5	36.9	21.2

Table 1. Semantic scene completion on Matterport3D [3] and ScanNet [9] collections. Our self-supervised method outperforms the supervised ScanComplete [12] in terms of mAcc measure.

set of 2D views $\{v\}$. Let ϕ_{seg} denote a function that maps an input RGB image I to per-pixel semantic labels S .

First, we pre-segment the *original captured* RGB-D images $\{(I_u, D_u), u \in U\}$ to obtain a set of accurate semantic labels $\{S_u^P\}$ (GT segmentations can also be used), that we refer to as *pseudo-ground-truth labels*, via $S_u^P = \phi_{\text{seg}}(I_u)$. We then compute a pseudo-supervised cross-entropy (CE) loss $\ell_{\text{seg-p}}$ between each pair of rendered \hat{S}_u and pseudo-GT S_u^P semantic views (see Figure 4 (a)):

$$\ell_{\text{seg-p},u} = \sum_p L_{\text{CE}}(\hat{S}_u(p), S_u^P(p)). \quad (3)$$

As the original RGB-D images are free from prediction artefacts, minimizing the pseudo-GT objective in (3) can provide a stable learning signal. However, the set of source views is finite, potentially limiting the supervision available to our model; additionally, excluding RGB photos would disable learning semantics entirely. We thus create a self-supervised training loop (see Figure 4 (b)) using only the predictions produced by our network. To this end, we randomly sample a set of viewing directions $V = \{v\}$ (see Section 4.1), render RGB \hat{I}_v and semantic \hat{S}_v images for each view, predict a segmentation $\hat{S}_v^R = \phi_{\text{seg}}(\hat{I}_v)$ for a rendered appearance view \hat{I}_v , and compute per-pixel cross-entropy between pairs (\hat{S}_v, \hat{S}_v^R) of respective semantic maps:

$$\ell_{\text{sem-r},v} = \sum_p L_{\text{CE}}(\hat{S}_v(p), \hat{S}_v^R(p)). \quad (4)$$

Unlike for the pseudo-supervised term (3), semantic maps \hat{S}_v^R in (4) need to be predicted on the fly for arbitrary rendered RGB images, requiring ϕ_{seg} to be a segmentation algorithm (e.g., a pre-trained network).

Output and Supervision Options. As ground-truth semantic labels are available for our datasets [3,9], we investigate several options for providing supervision to our model and compare between 3D GT labels, 2D GT labels, and 2D pseudo-GT labels. Our semantic predictor ϕ_{seg} , is a pre-trained MSeg semantic segmentation network [30]. We find that using pseudo-GT labels in our experiments leads to a

Method	Recall	IoU
ScanComplete [12] (<i>sup.</i>)	36	30
SG-NN [10] (<i>self-sup.</i>)	57	28
SPSG [13] (<i>self-sup.</i>)	64	39
Ours (<i>self-sup., pseudo-GT</i>)	63	34

Table 2. Geometry completion results on Matterport3D. Our self-supervised method outperforms the supervised ScanComplete [12] in terms of accuracy measure.

moderate decrease in segmentation performance, and report quantitative results in Section 4.3.

Summary. Our final training objective integrates geometry, color, and semantic terms

$$L = \sum_{u \in U} \frac{1}{n_u} [\ell_{\text{geo},u} + \ell_{\text{app},u} + \ell_{\text{seg-p},u}] + \sum_{v \in V} \frac{1}{n_v} \ell_{\text{sem-r},v},$$

over the set of n_u (n_v) valid pixels in U (V) (i.e., pixels where surface geometry was predicted in \hat{d}), and the 3D term of the form $\sum_{\text{chunks}} \ell_{\text{geo-3d}}$. To calculate the loss terms in the 2D domain, we use a 3D volumetric mask of the form $\{x : \hat{d}(x) < \varepsilon\}$ (we use $\varepsilon = 3$ cm) corresponding to the generated geometry, available upon completing geometry in each voxel of the input volumetric grid.

4. Experiments

4.1. Experimental Setup

To evaluate our system and validate our design choices, we conduct a series of experiments, predominantly using large-scale real 3D scans in the Matterport3D collection [3], reporting additional results on ScanNet [9]. Both collections provide abundant real-world training/testing data; following the official train/val/test split of Matterport3D (1788/394 rooms for train/val/test) and ScanNet dataset (1201/312 rooms for train/val). To obtain highly detailed reconstructions, we use fine, 2 cm voxels during TSDF fusion; for saving memory during training, we extract $64 \times 64 \times 128$ subvolumes from fused scans. We use 77,581 and 88,420 chunks for training with Matterport3D and ScanNet respectively. Following prevailing practice [10, 12, 13, 24, 29], we report mean intersection-over-union (mIoU) and mean voxelwise accuracy (mAcc) measures for semantic segmentation and IoU and Recall for geometry completion. To enable the fully self-supervised training for 3D semantics, we use a pre-trained MSeg model [30] to generate pseudo-labels for the 2D images from Matterport3D and ScanNet datasets. Following ScanComplete [12], we map the pre-defined 196 universal classes in MSeg into most frequently

Method	Part.-to-part.		Full-to-full	
	mAcc	mIoU	mAcc	mIoU
ScanComplete [12] (<i>sup.</i>)	46.6	35.8	42.1	29.7
BPNNet [23] (<i>sup.</i>)	47.7	33.3	41.1	32.2
3D CNN (<i>sup.</i>)	50.9	39.5	46.3	33.5
VMF [28] (<i>pseudo-fusion</i>)	—	—	24.9	17.6
Ours (<i>self-sup.</i> , <i>pseudo-GT</i>)	33.9	26.2	32.9	20.4

Table 3. Semantic segmentation results on Matterport3D. In this context, we provide the first self-supervised semantic segmentation results.

occurring categories (11 for Matterport3D and 15 for ScanNet). Quantitatively, our pre-trained predictor demonstrates a mean IoU performance of, specifically, 36.9% for Matterport3D and 37.4% for ScanNet (on training split).

Training with Virtual View Selection. During training, we on-the-fly generate additional, virtual views independent to the original views in our data, to provide auxiliary semantic supervision. A similar technique is proposed in [29], yielding improved performance of a semantic 3D mesh segmentation by sampling views with otherwise unusual directions and fields of view. For us, one constraint of the original images is their field of view as many are taken close to objects or walls, lacking objects’ features and context necessary for accurate segmentation. To remedy this issue, we (1) use a camera model with wider field of view, providing larger spatial context, leading to more accurate semantic segmentation, and (2) sample camera poses with more object content, pulling the camera away from objects. We give more details in the supplemental.

4.2. Comparisons to State-of-the-Art

Semantic Scene Completion. As a semantic scene completion baseline, we use ScanComplete [12], a supervised method operating on 3D TSDF volumes. In the context of geometry completion, we additionally compare to the self-supervised SG-NN [10] and SPSPG [13] baselines; we note that these methods do not perform semantic segmentation. For reference in either evaluation, we report performance achieved using a fully-supervised baseline approach 3D CNN. We note that among these methods, ScanComplete and SPSPG perform complex multi-modal training like our method while SG-NN focuses on completion only.

We present the results statistically in Tables 1–2 for Matterport3D and ScanNet; visual comparison is presented in Figure 5 and compares semantic reconstructions obtained for ScanNet datasets. We note that in terms of voxelwise accuracy of both semantics and geometry completion measures, our method achieves similar or improved performance compared to ScanComplete approach.

Method	mAcc	mIoU
3D CNN (<i>sup.</i>)	49.7	34.4
3D CNN w/o color dec. (<i>sup.</i>)	48.2	33.6
3D CNN w/o color enc. (<i>sup.</i>)	45.1	30.1
VMF [28] (<i>pseudo fusion</i>)	24.9	17.6
Ours (<i>self-sup.</i> , <i>pseudo-GT</i>)	35.3	21.5
Ours + 2D GT (<i>self-sup.</i>)	44.8	28.6

Table 4. Ablative study on 2D color encoder/decoder in terms of semantic scene reconstruction on Matterport3D.

For completing geometry, our approach outperforms the self-supervised SG-NN (presumably, due to color input) but demonstrates slightly inferior quantitative performance compared to SPSPG; we attribute this to a side effect of multi-modal training with pseudo-labels.

Semantic Segmentation (without Completion). For reference, we additionally evaluate semantic labeling in isolation, without performing geometry completion, operating instead on a given (possibly, incomplete) scene. We provide semantic segmentation results on Matterport3D in Table 3 and Figure 6. In this case, all our networks were trained for both completion and segmentation, and only evaluated in a setting focused on segmentation. Please note that, to make a fair comparison, we implemented VMF [29] and used the same 2D pseudo semantic labels to ours for inference. 3D segmentation is obtained by back-projecting and fusing 2D pseudo labels with ground truth depths and camera poses. This further highlights the effectiveness of our approach by bridging 3D and 2D observations compared to purely view-based approaches.

4.3. Ablative Studies

What is the effect of pseudo-labeling? We quantitatively study the effect of having access to true GT labels compared to using pseudo-GT labels predicted by a generic network, on semantic reconstruction performance. Results in Table 3 suggest that substituting pseudo-labels for GT amounts to a significant boost in quality: 9.5% mean accuracy and 7.1% mean IoU improvement. Further, we take a closer look at fully supervised training with 3D CNN network of the type we used, and whether color information is instrumental in achieving good quality. We find that in fact, our 3D CNN architecture enables to achieve the new state-of-the-art semantic scene completion performance. Removing color decoder/supervision amounts to 0.8% mean IoU reduction; most importantly, removing access to color inputs degrades performance by 3.3% mean IoU.

What is the effect of color supervision? We investigate the influence of color information integrated into the 3D network at different levels for training on semantic recon-

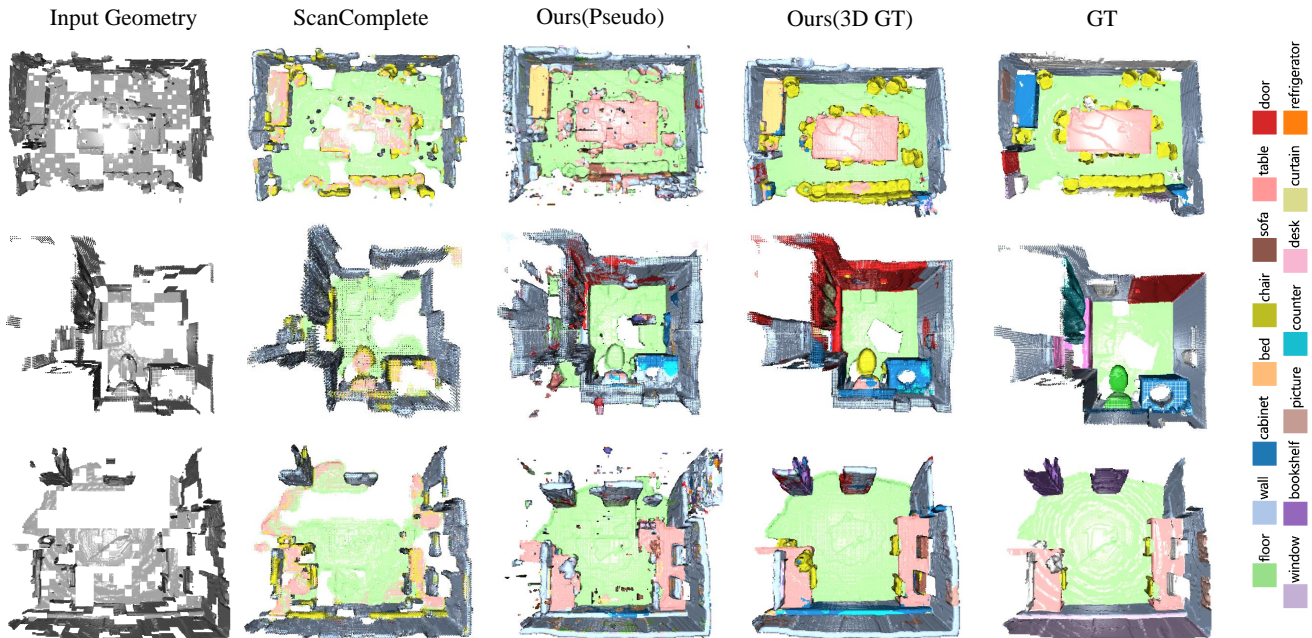


Figure 5. Semantic scene completion results using the ScanNet collection reveal that our self-supervised approach is able to inpaint gaps and perform segmentation favourably to the supervised ScanComplete [12] method.

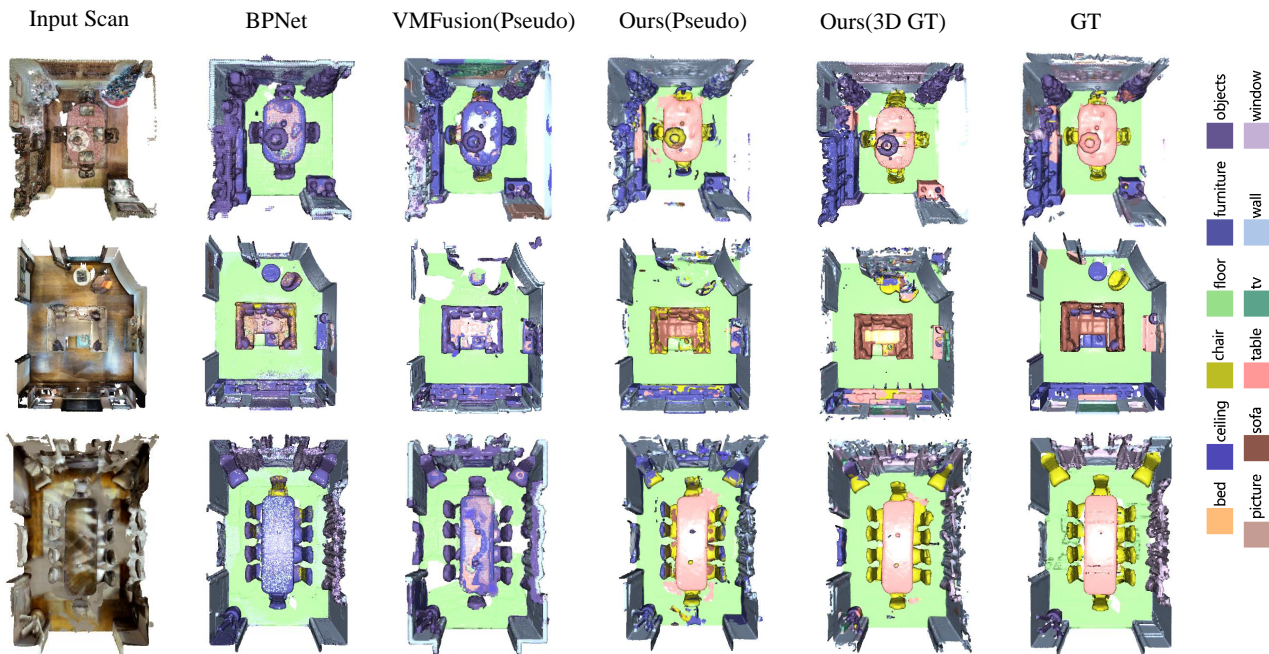


Figure 6. Qualitative semantic segmentation results using our approach and supervised competitor methods [24, 29] on Matterport3D dataset. Compared to the baselines, our approach demonstrates robust performance; a 3D supervised variant is able to achieve state-of-the-art results.

struction results. Generally, as NNs can easily leverage heterogeneous information, having more diverse inputs boosts

performance as shown in Table 4, which presents semantic scene reconstruction results by ablating the color encoder

Method	Part.-to-part.		Full-to-full		Part.-to-full	
	mAcc	mIoU	mAcc	mIoU	mAcc	mIoU
Ours (<i>pseudo-GT</i>)	33.9	26.2	32.9	20.4	35.3	21.5
Ours + 2D GT	46.3	32.8	39.3	26.2	44.8	28.6
Ours + 2D GT, w/o compl.	39.4	28.6	35.5	24.2	—	—

Table 5. Ablative study of semantic scene reconstruction on Matterport3D with different completeness for input and output for evaluation. The designation *Partial-to-partial* means we take a partial scan as input and evaluate the semantic results on the input partial scan, and *Full-to-full* means we take a full scan as input and evaluate the semantic results on the full scan; *Partial-to-full* scheme denotes we take a partial scan as input but evaluate the semantic results on full scan.

and decoder. We demonstrate that new state-of-the-art results can be achieved with the help of fully supervised learning, which we report as an upper bound of our method.

What is the effect of varying inputs and supervision? We more closely investigate the effect of having more complete or incomplete inputs during training, and training our model in self-supervised way without having to perform geometry completion. Table 5 presents semantic scene reconstruction results with different levels of completeness for input and output. Our experiments demonstrate that the scene completion task elevates the semantic segmentation task. Taking a partial scan as input and simultaneously performing scene completion and semantic segmentation outperforms the ones that we purely train the network with only the segmentation head taking a complete scene or a partial scene as input.

5. Conclusion

We have presented the first to date algorithm to learn geometry completion, scan colorization, and semantic segmentation in a single, self-supervised training procedure. Our approach to self-supervised learning builds on several crucial design choices, most importantly, an efficient multi-modal deep neural U-network with residual blocks, a differentiable rendering technique augmented to produce semantic maps, and progress in universal semantic pretraining. Fundamentally, our approach enables joint geometry and color reconstruction as well as semantic labeling for unseen scenes without requiring ground-truth labels, a stepping stone in building accurate, semantic models of real-world environments. We have additionally established that adding ground-truth information where it is available considerably improves semantic reconstruction performance; in fact, leveraging 3D ground-truth enables achieving state-of-the-art results.

References

- [1] Iro Armeni, Sasha Sax, Amir R Zamir, and Silvio Savarese. Joint 2d-3d-semantic data for indoor scene understanding. *arXiv preprint arXiv:1702.01105*, 2017. 2
- [2] Yingjie Cai, Xuesong Chen, Chao Zhang, Kwan-Yee Lin, Xiaogang Wang, and Hongsheng Li. Semantic scene completion via integrating instances and scene in-the-loop. In *Proceedings of the IEEE/CVF Conference on Computer Vision and Pattern Recognition*, pages 324–333, 2021. 2, 3
- [3] Angel Chang, Angela Dai, Thomas Funkhouser, Maciej Halber, Matthias Niebner, Manolis Savva, Shuran Song, Andy Zeng, and Yinda Zhang. Matterport3d: Learning from rgb-d data in indoor environments. In *International Conference on 3D Vision*, pages 667–676. IEEE, 2017. 1, 2, 5, 6
- [4] Yujin Chen, Matthias Nießner, and Angela Dai. 4dcontrast: Contrastive learning with dynamic correspondences for 3d scene understanding. In *European Conference on Computer Vision*, 2022. 2
- [5] Christopher Choy, JunYoung Gwak, and Silvio Savarese. 4d spatio-temporal convnets: Minkowski convolutional neural networks. In *Proceedings of the IEEE/CVF Conference on Computer Vision and Pattern Recognition*, pages 3075–3084, 2019. 2
- [6] Özgün Çiçek, Ahmed Abdulkadir, Soeren S Lienkamp, Thomas Brox, and Olaf Ronneberger. 3d u-net: learning dense volumetric segmentation from sparse annotation. In *International conference on medical image computing and computer-assisted intervention*, pages 424–432. Springer, 2016. 4
- [7] Jonathan Crespo, Jose Carlos Castillo, Oscar Martinez Mozos, and Ramon Barber. Semantic information for robot navigation: A survey. *Applied Sciences*, 10(2):497, 2020. 2
- [8] Brian Curless and Marc Levoy. A volumetric method for building complex models from range images. In *Proceedings of the 23rd annual Conference on Computer Graphics and Interactive Techniques*, pages 303–312, 1996. 4
- [9] Angela Dai, Angel X Chang, Manolis Savva, Maciej Halber, Thomas Funkhouser, and Matthias Nießner. Scannet: Richly-annotated 3d reconstructions of indoor scenes. In *Proceedings of the IEEE Conference on Computer Vision and Pattern Recognition*, pages 5828–5839, 2017. 2, 5, 6
- [10] Angela Dai, Christian Diller, and Matthias Nießner. Sg-nn: Sparse generative neural networks for self-supervised scene completion of rgb-d scans. In *Proceedings of the IEEE/CVF Conference on Computer Vision and Pattern Recognition*, pages 849–858, 2020. 2, 3, 6, 7
- [11] Angela Dai and Matthias Nießner. 3dmv: Joint 3d-multi-view prediction for 3d semantic scene segmentation. In *Proceedings of the European Conference on Computer Vision*, pages 452–468, 2018. 2
- [12] Angela Dai, Daniel Ritchie, Martin Bokeloh, Scott Reed, Jürgen Sturm, and Matthias Nießner. Scancomplete: Large-scale scene completion and semantic segmentation for 3d scans. In *Proceedings of the IEEE Conference on Computer Vision and Pattern Recognition*, pages 4578–4587, 2018. 2, 3, 6, 7, 8

- [13] Angela Dai, Yawar Siddiqui, Justus Thies, Julien Valentin, and Matthias Nießner. Spsg: Self-supervised photometric scene generation from rgb-d scans. In *Proceedings of the IEEE/CVF Conference on Computer Vision and Pattern Recognition*, pages 1747–1756, 2021. 2, 4, 5, 6, 7
- [14] Aloisio Dourado, Frederico Guth, and Teofilo de Campos. Data augmented 3d semantic scene completion with 2d segmentation priors. In *Proceedings of the IEEE/CVF Winter Conference on Applications of Computer Vision*, pages 3781–3790, 2022. 2, 3
- [15] Guoguang Du, Kai Wang, Shiguo Lian, and Kaiyong Zhao. Vision-based robotic grasping from object localization, object pose estimation to grasp estimation for parallel grippers: a review. *Artificial Intelligence Review*, 54(3):1677–1734, 2021. 2
- [16] Xiao Fu, Shangzhan Zhang, Tianrun Chen, Yichong Lu, Lanyun Zhu, Xiaowei Zhou, Andreas Geiger, and Yiyi Liao. Panoptic nerf: 3d-to-2d label transfer for panoptic urban scene segmentation. *arXiv preprint arXiv:2203.15224*, 2022. 4
- [17] Kyle Genova, Xiaoqi Yin, Abhijit Kundu, Caroline Pantofaru, Forrester Cole, Avneesh Sud, Brian Brewington, Brian Shucker, and Thomas Funkhouser. Learning 3d semantic segmentation with only 2d image supervision. In *International Conference on 3D Vision*, pages 361–372. IEEE, 2021. 2, 3
- [18] Yuxiao Guo and Xin Tong. View-volume network for semantic scene completion from a single depth image. In *Proceedings of the 27th International Joint Conference on Artificial Intelligence*, pages 726–732, 2018. 3
- [19] Abdul Mueed Hafiz and Ghulam Mohiuddin Bhat. A survey on instance segmentation: state of the art. *International journal of multimedia information retrieval*, 9(3):171–189, 2020. 2
- [20] Kaiming He, Xiangyu Zhang, Shaoqing Ren, and Jian Sun. Deep residual learning for image recognition. In *Proceedings of the IEEE conference on computer vision and pattern recognition*, pages 770–778, 2016. 4
- [21] Ji Hou, Angela Dai, and Matthias Nießner. 3d-sis: 3d semantic instance segmentation of rgb-d scans. In *Proceedings of the IEEE/CVF Conference on Computer Vision and Pattern Recognition*, pages 4421–4430, 2019. 2
- [22] Ji Hou, Angela Dai, and Matthias Nießner. Revealnet: Seeing behind objects in rgb-d scans. In *Proceedings of the IEEE/CVF Conference on Computer Vision and Pattern Recognition*, pages 2098–2107, 2020. 2, 3
- [23] Ji Hou, Benjamin Graham, Matthias Nießner, and Saining Xie. Exploring data-efficient 3d scene understanding with contrastive scene contexts. In *Proceedings of the IEEE/CVF Conference on Computer Vision and Pattern Recognition*, pages 15587–15597, 2021. 2
- [24] Wenbo Hu, Hengshuang Zhao, Li Jiang, Jiaya Jia, and Tien-Tsin Wong. Bidirectional projection network for cross dimension scene understanding. In *Proceedings of the IEEE/CVF Conference on Computer Vision and Pattern Recognition*, pages 14373–14382, 2021. 2, 6, 8
- [25] Hiroharu Kato, Deniz Beker, Mihai Morariu, Takahiro Ando, Toru Matsuoka, Wadim Kehl, and Adrien Gaidon. Differentiable rendering: A survey. *arXiv preprint arXiv:2006.12057*, 2020. 5
- [26] Salman Khan, Muzammal Naseer, Munawar Hayat, Syed Waqas Zamir, Fahad Shahbaz Khan, and Mubarak Shah. Transformers in vision: A survey. *ACM computing surveys (CSUR)*, 54(10s):1–41, 2022. 2
- [27] Alexander Kirillov, Kaiming He, Ross Girshick, Carsten Rother, and Piotr Dollár. Panoptic segmentation. In *Proceedings of the IEEE/CVF Conference on Computer Vision and Pattern Recognition*, pages 9404–9413, 2019. 2
- [28] Abhijit Kundu, Kyle Genova, Xiaoqi Yin, Alireza Fathi, Caroline Pantofaru, Leonidas J Guibas, Andrea Tagliasacchi, Frank Dellaert, and Thomas Funkhouser. Panoptic neural fields: A semantic object-aware neural scene representation. In *Proceedings of the IEEE/CVF Conference on Computer Vision and Pattern Recognition*, pages 12871–12881, 2022. 4
- [29] Abhijit Kundu, Xiaoqi Yin, Alireza Fathi, David Ross, Brian Brewington, Thomas Funkhouser, and Caroline Pantofaru. Virtual multi-view fusion for 3d semantic segmentation. In *European Conference on Computer Vision*, pages 518–535. Springer, 2020. 2, 6, 7, 8
- [30] John Lambert, Zhuang Liu, Ozan Sener, James Hays, and Vladlen Koltun. MSeg: A composite dataset for multi-domain semantic segmentation. In *Proceedings of the IEEE/CVF Conference on Computer Vision and Pattern Recognition*, 2020. 2, 6
- [31] Wenbin Li, Sajad Saeedi, John McCormac, Ronald Clark, Dimos Tzoumanikas, Qing Ye, Yuzhong Huang, Rui Tang, and Stefan Leutenegger. Interiornet: Mega-scale multi-sensor photo-realistic indoor scenes dataset. In *British Machine Vision Conference*, 2018. 2
- [32] Jenny Lin, Xingwen Guo, Jingyu Shao, Chenfanfu Jiang, Yixin Zhu, and Song-Chun Zhu. A virtual reality platform for dynamic human-scene interaction. In *SIGGRAPH ASIA 2016 virtual reality meets physical reality: Modelling and simulating virtual humans and environments*, pages 1–4, 2016. 1
- [33] Shengyi Qian, Alexander Kirillov, Nikhila Ravi, Deendra Singh Chiplot, Justin Johnson, David F Fouhey, and Georgia Gkioxari. Recognizing scenes from novel viewpoints. *arXiv preprint arXiv:2112.01520*, 2021. 3
- [34] Shuran Song, Fisher Yu, Andy Zeng, Angel X Chang, Manolis Savva, and Thomas Funkhouser. Semantic scene completion from a single depth image. In *Proceedings of the IEEE conference on computer vision and pattern recognition*, pages 1746–1754, 2017. 2, 3
- [35] Peng-Shuai Wang, Yang Liu, and Xin Tong. Deep octree-based cnns with output-guided skip connections for 3d shape and scene completion. In *Proceedings of the IEEE/CVF Conference on Computer Vision and Pattern Recognition Workshops*, pages 266–267, 2020. 3
- [36] Yida Wang, David Joseph Tan, Nassir Navab, and Federico Tombari. Forknet: Multi-branch volumetric semantic completion from a single depth image. In *Proceedings of the IEEE/CVF International Conference on Computer Vision*, pages 8608–8617, 2019. 2, 3

- [37] Zongji Wang and Feng Lu. Voxsegnet: Volumetric cnns for semantic part segmentation of 3d shapes. *IEEE transactions on visualization and computer graphics*, 26(9):2919–2930, 2019. 2
- [38] Saining Xie, Jiatao Gu, Demi Guo, Charles R Qi, Leonidas Guibas, and Or Litany. Pointcontrast: Unsupervised pre-training for 3d point cloud understanding. In *European conference on computer vision*, pages 574–591. Springer, 2020. 2
- [39] Yuxing Xie, Jiaojiao Tian, and Xiao Xiang Zhu. Linking points with labels in 3d: A review of point cloud semantic segmentation. *IEEE Geoscience and Remote Sensing Magazine*, 8(4):38–59, 2020. 2
- [40] Lior Yariv, Jiatao Gu, Yoni Kasten, and Yaron Lipman. Volume rendering of neural implicit surfaces. *Advances in Neural Information Processing Systems*, 34:4805–4815, 2021. 5
- [41] Jiahui Zhang, Hao Zhao, Anbang Yao, Yurong Chen, Li Zhang, and Hongen Liao. Efficient semantic scene completion network with spatial group convolution. In *Proceedings of the European Conference on Computer Vision*, pages 733–749, 2018. 3
- [42] Pingping Zhang, Wei Liu, Yinjie Lei, Huchuan Lu, and Xiaoyun Yang. Cascaded context pyramid for full-resolution 3d semantic scene completion. In *Proceedings of the IEEE/CVF International Conference on Computer Vision*, pages 7801–7810, 2019. 3
- [43] Yifei Zhang, Désiré Sidibé, Olivier Morel, and Fabrice Mériaudeau. Deep multimodal fusion for semantic image segmentation: A survey. *Image and Vision Computing*, 105:104042, 2021. 2
- [44] Shuaifeng Zhi, Tristan Laidlow, Stefan Leutenegger, and Andrew J Davison. In-place scene labelling and understanding with implicit scene representation. In *Proceedings of the IEEE/CVF International Conference on Computer Vision*, pages 15838–15847, 2021. 4